

A Multimodal and Pathological Analysis of a Renal Cell Carcinoma Metastasis to the Thyroid Gland 11 Years Post Nephrectomy

Thomas Rand Geisbush^{1*}, Zaneta Dymon³, Medhat Sam Gabriel³, Vivek Yedavalli²

1. Chicago Medical School, Rosalind Franklin University of Medicine and Science, North Chicago, USA

2. Department of Neuroimaging and Neurointervention, Stanford Hospital, Palo Alto, USA

3. Department of Radiology, Loyola University Medical Center, Illinois, USA

* **Correspondence:** Tom Geisbush, MD, 2757 Matera Lane, San Diego, CA, 92108, USA
(✉ thomas.geisbush@my.rfums.org)

Radiology Case. 2019 Apr; 13(4):1-9 :: DOI: 10.3941/jrcr.v13i4.3497

ABSTRACT

Thyroid lesions have a comprehensive differential diagnosis which include benign and malignant entities, such as metastases. However, metastases only account for a small percentage of thyroid lesions with renal cell carcinoma as the most common. Metastases to the thyroid pose a diagnostic dilemma as symptoms may not manifest for up to decades after removal of the renal cell carcinoma. Due to the nonspecific appearance on computed tomography and ultrasound, distinguishing metastases from primary thyroid malignancies is of the utmost importance for timely patient management. Our case demonstrates the importance of considering RCC metastases to the thyroid even years after nephrectomy to mitigate potential delays in diagnosis. We present the case of a 66-year-old male with a past medical history of renal cell carcinoma status post nephrectomy 11 years prior who demonstrated incidental thyroid abnormalities on positron emission tomography/computed tomography and ultrasound later confirmed as a metastasis of renal cell carcinoma.

CASE REPORT

CASE REPORT

Our case involves a 66-year-old male with a past medical history of renal cell carcinoma (RCC) status post complete left nephrectomy 11 years prior in 2004 who presented with chest pain in 2015. Positron emission tomography/computed tomography (PET/CT) demonstrated a hypermetabolic focus in the left thyroid lobe with a maximum standard uptake value (max SUV) of 8.6 (Figure 1). The lesion was initially suspected to be a new primary malignancy. However,

parathyroid hormone, thyroid stimulating hormone, T3, and T4 levels were within normal limits.

PET/CT was performed for attenuation correction and anatomic localization. An additional nonenlarged, left, level 3 hypermetabolic focus posterolateral to the left thyroid lobe was noted (max SUV 3.5) suggestive of metastatic lymphadenopathy (Figure 1). Color Doppler ultrasonography was then performed showing a heterogenous, hypoechoic nodule in the lower-mid pole of the left lobe measuring 3.3 cm x 1.6 cm x 1.4 cm in size with central hypervascularity (Figure

2). Fine needle aspiration (FNA) of the nodule was performed and subsequent CD10 positive staining of the pathologic specimen found the mass compatible with RCC origin (Figure 3). Patient was started on palliative radiation therapy to the thyroid shortly afterwards due to compression of the internal jugular vein. Follow up CT imaging with contrast showed a hypodense appearance of both thyroid lobes with irregular peripheral enhancement (Figure 4). The right lobe hypodensity was larger measuring 3.3 cm x 2.5 cm x 4.6 cm. Findings were consistent with metastatic involvement and internal necrosis of both thyroid lobes.

DISCUSSION

Despite its robust vascularity, metastases to the thyroid gland only account for a small proportion of benign and malignant thyroid entities diagnosed. The correct diagnosis and management of metastases to the thyroid can be further delayed due to their nonspecific and commonly benign characteristics on CT and ultrasound imaging. Confirming the diagnosis of metastases to the thyroid requires specific techniques on pathology that may not be employed without the proper communication between radiologists, clinicians, and pathologists about the possibility of metastatic disease. Therefore, it is important to keep metastases to the thyroid within the differential of a patient that has a known history of primary malignancy.

ETIOLOGY & DEMOGRAPHICS:

RCC is the most common of all primary malignancies to metastasize to the thyroid although primary lesions to the thyroid are much more prevalent in general [1], [2]. Reviews of the literature found thyroid metastases to account for only 1.3% to 3% of all clinical thyroid malignancies although autopsy series have reported incidence of nonclinical thyroid metastases as high as 22.4 % [1], [4]. Sindoni et al. found the incidence of metastases to the thyroid from RCC reported between 10% to 34% [5]. A review of metastases to the thyroid diagnosed with FNA found both renal and lung to be the most frequent primary malignancy site (22% respectively) [1]. Chung et al. found renal cell malignancies to be the source of metastases to the thyroid 48.1% of the time [2]. The female to male ratio of RCC metastases to the thyroid has been reported as 1.35:1 respectively [5]. RCC metastases most commonly appear in the 6th and 7th decades of life and often occur months to years after the primary tumor has occurred (metachronous) [5]. The time frame in which metachronous metastases can arise from RCC varies. Metastases have been reported from as early as a few months to as late as 30 years after nephrectomy [3], [5]. Case series have shown the average time from primary malignancy to metastases to be 9.1 – 9.4 years [1], [4]. The prevalence of severely delayed metastases even after nephrectomy for RCC speaks to why it is important to include RCC metastases in the differential of a thyroid lesion even after years since primary malignancy.

RCC spreads through both hematogenous and lymphatic routes. It mainly metastasizes to lung, bone, liver, adrenals glands, brain, and skin [6]. However, RCC is also notorious for metastasizing to uncommon locations. Although the thyroid

gland is a highly vascularized structure, it is an uncommon site of metastatic disease. The high level of oxygen and iodine content have been postulated to create an inhospitable environment for incoming tumor cells as well as the high velocity blood flow within the thyroid vasculature [4]. It has been further hypothesized that when the integrity of normal thyroid is compromised due to a benign or malignant entity, decreases in levels of iodine and oxygen, along with abnormalities in normal blood flow, can contribute to the rise of metastatic disease. Such disturbances to normal thyroid structure can result from benign growths such as multinodular goiter or follicular adenoma. Moreover, these abnormalities can also result from malignant tumor growth with metastatic spread leading to a tumor-in-tumor pattern [2], [7], [8].

CLINICAL & IMAGING FINDINGS:

RCC metastasis most commonly presents as a solitary solid mass within the thyroid mimicking the more common primary thyroid neoplasms [4]. The presentation of RCC metastasis to the thyroid can vary significantly. Chung et al. found that among all metastases to the thyroid, the majority (74.9%) presented with clear clinical manifestations such as neck mass, swelling, and dysphagia while a minority (25.1%) of cases were incidentally found on physical exam or imaging studies [2]. In previous case studies specifically involving RCC metastases to the thyroid, clinical symptoms have also included cervical pain, hoarseness, cough, wheezing, painless nodules and breathing difficulties [9], [10], [11]. Swelling due to RCC metastasis has even resulted in acute airway failure requiring emergent intubation [12].

Imaging characteristics can be relatively nonspecific for differentiating between RCC metastases and primary thyroid neoplasms. Indeed, before pathological analysis confirmed metastasis, several cases have been reported where the thyroid lesions were initially thought to be primary in nature [13].

The ultrasonographic imaging characteristics also present with findings that are usually indistinguishable from more common primary pathology of the thyroid. A majority of RCC metastases are sonographically solid, hypoechoic, internally hypervascular, and without calcification. However, cases have been reported where the lesion demonstrates little hypervascularity and presents with characteristics of a more benign entity [14]. Different case series have described RCC metastases as both having an irregular or ovoid shape on ultrasound [15]-[16]. Although not detected in our patient, a distinct ultrasound feature was described in 4 out of 10 patients studied with metastatic lesions 25-81mm x 19-41mm x 19-70mm in size where echogenic tumor thrombus protruding into the thyroid and internal jugular vein could be visualized as an “echogenic tongue” [15]. There has been some limited use of ultrasound elastography to study RCC metastases to the thyroid [17-18]. Using Quasi-static elastography, a quantitative measure of the relative stiffness of the lesion to normal thyroid tissue (strain ratio) showed an RCC metastasis to be three times harder than normal thyroid tissue [17]. Using Shear-wave elastography, where elasticity is directly calculated by measuring the speed of wave propagation through the tissue, an RCC metastasis was also measured three times as hard as normal thyroid tissue although the value range

also overlapped with that of benign thyroid lesions [17]. Conversely, RCC metastasis to the thyroid have also been described as relatively elastic compared to more characteristically “hard” neoplastic thyroid lesions [18]. These conflicting reports using ultrasound elastography to investigate the properties on RCC metastases to the thyroid indicate that more research into this modality may be required. CT with contrast imaging findings of metastatic versus primary thyroid malignancies are nonspecific. Previous reports with CT imaging show similar characteristics to our current report with central hypodensity and peripheral enhancement, suggesting internal necrosis of thyroid tissue [14], [19], [20]. While the use of PET/CT has not been shown to reliably diagnose primary RCC, a recent meta-analysis showed PET/CT to have a sensitivity of 0.86 and a specificity of 0.88 for restaging of RCC and detection of distant metastases [21]. However, these studies did not pertain specifically to detection of thyroid lesions. Malignant versus benign thyroid lesions are commonly differentiated by the distribution and intensity of FDG uptake with malignant lesions characteristically presenting with more focal and intense uptake compared to benign lesions [22]. However, to our knowledge the ability of PET/CT to differentiate an RCC metastasis to the thyroid versus other primary thyroid neoplasms has not been specifically studied. Detection of incidental thyroid lesions on PET/CT that turned out to be renal cancer metastases to the thyroid in previous case studies were confirmed by histopathological analysis and did not comment on specific imaging characteristics differentiating the metastases from other primary thyroid neoplasms [20], [23]. Metastatic nodules are also characteristically “cold” nodules on scintigraphy, although exceptions have been reported [24]. While magnetic resonance imaging (MRI) has not been described to our knowledge to assess RCC metastases to the thyroid, recent evidence of the use of apparent diffusion coefficient (ADC) values to differentiate malignant versus benign solitary thyroid nodules has shown some promise [25]. The use of MRI and ADC values in identifying metastases to the thyroid could warrant further investigation.

Definitive diagnosis of metastatic RCC to the thyroid can only be confirmed by immunohistochemical staining and histologic examination. FNA with ultrasound guidance is the most common approach. FNA sensitivity and specificity for diagnosing metastases to the thyroid have been reported to be as high as 94% and 100% [1]. However, other reviews have shown preoperative FNA of the thyroid for a metastasis gave the incorrect diagnosis 26.3% of the time, of which RCC had the highest inaccuracy rate of all (28.6%) [2]. Song et al. looked at the use of FNA in comparison to core needle biopsy (CNB) in diagnosing RCC metastases to the thyroid and found that only one nodule from their sample (11.8%) was confirmed as metastatic RCC with FNA, while all CNBs were able to correctly diagnose all RCC metastases (9/9) without further follow up [16]. When a metastasis is suspected, pathology needs to be alerted so immunohistochemical staining for markers specific to RCC are utilized including CD10, vimentin, cytokeratin 7, and renal cell carcinoma marker [26]. It is also informative to use staining markers for thyroglobulin, calcitonin, and thyroid transcription factor 1 (TTF-1), which

are specific to primary thyroid carcinomas and negative with metastatic RCC.

TREATMENT & PROGNOSIS:

Total or partial thyroidectomy is appropriate for eligible candidates once the diagnosis of RCC metastasis to thyroid has been confirmed. Patients with limited or solitary metastases usually have a good prognosis post resection, and even those with more diffuse metastases require thyroidectomy for palliative measures concerning compression and discomfort. A recent study of patient status post thyroidectomy showed the overall 5-year survival rate to be 46% with 26% of patients developing neck recurrence at a median of 12 months after thyroidectomy [27]. If patients are not surgical candidates, medical therapies including immunotherapy, multi-kinase inhibitors, anti-vascular endothelial growth factor (VEGF) agents, and mammalian target of rapamycin inhibitors which can be used to inhibit cell replication and proliferation by inhibiting the mechanistic target of rapamycin cell (mTOR) signaling pathway.

DIFFERENTIAL DIAGNOSIS:

PAPILLARY THYROID CARCINOMA:

Papillary thyroid carcinoma is the most common primary thyroid malignancy accounting for approximately 70% of all thyroid malignancies [28]. Ultrasound imaging shows a nodular, ill-defined border with solid internal architecture, increased internal vascularity, small echogenic foci representing microcalcifications (psammoma bodies) [29]-[30]. Hypoechoic, cystic components and larger macrocalcifications may also be present in certain variants [30]. CT imaging shows a dense mass with heterogenous hyperdensities representing internal microcalcifications [31]. Lymph node involvement is commonly discovered on CT imaging [32]. Papillary thyroid carcinoma has been shown to have variable FDG uptake with higher FDG avidity possibly associated with specific genetic mutations [33].

FOLLICULAR THYROID NEOPLASM:

Both benign or malignant follicular neoplasms are indistinguishable on imaging and must be surgically resected for definitive diagnosis. On ultrasound follicular neoplasms are usually uniform, hypoechoic nodules that can be easily differentiated from normal surrounding thyroid tissue [30]. Poorly differentiated variants can exhibit a more ill-defined margin without normal adjacent tissue [30]. CT imaging is relatively nonspecific showing a hypo- to isodense mass. On PET poorly differentiated subtypes of follicular neoplasm have been shown to correlate with increased FDG uptake likely due to upregulated glucose 1 transporter expression [34].

MEDULLARY THYROID CARCINOMA:

Medullary thyroid carcinoma arises from the parafollicular C-cells of the thyroid and characteristically secretes calcitonin [34]. On ultrasound medullary thyroid carcinoma appears as a solid, nodular structure with ill-defined lateral margins and can exhibit extracapsular extension [30]. Large, coarse hyperechoic calcifications can be present [32]. CT commonly shows a hypodense mass with possible large hyperdensities representing coarse macrocalcifications [32]. The use of measuring FDG uptake for medullary thyroid

carcinoma has not been shown to be useful for diagnosis or staging of the disease with studies showing max SUV overlap between progressive and stable disease [34]. PET/CT has shown some utility in evaluating for lymph node involvement [34].

ANAPLASTIC THYROID CARCINOMA:

Anaplastic thyroid carcinoma is an aggressive, undifferentiated tumor that primarily affects the elderly and has a poor prognosis compared to other primary malignancies of the thyroid. Ultrasound characteristics include a heterogenous, infiltrative appearance with possible hyperechoic foci representing microcalcifications [31]. On CT anaplastic thyroid carcinoma can present as a large, solid, infiltrative mass with internal hypodense regions representing necrosis and occasional hyperdense regions representing calcification [35]. Anaplastic thyroid carcinoma has a characteristically high glucose metabolism which results in avid FDG uptake [34].

THYROID LYMPHOMA:

Thyroid lymphoma constitutes approximately 1 - 5% of thyroid malignancies [34]. On ultrasound thyroid lymphoma is characteristically diffuse and heterogenous with marked regions of hypoechoogenicity [32]. Signs of infiltration and extracapsular extension can be seen [30]. On CT thyroid lymphoma shows diffuse, heterogenous density with replacement of normal thyroid parenchyma [30]. Displacement of airway and vascular structures is common [30]. Thyroid lymphoma exhibits avid FDG uptake [34].

TEACHING POINT

It is important to consider metastatic RCC in the setting of a new thyroid lesion resembling primary thyroid malignancy on imaging even years after nephrectomy. Since specific immunohistochemical staining is required to diagnose RCC metastases, consideration and proper communication with other health care professionals are required to mitigate the risk of a delayed diagnosis.

REFERENCES

1. Hegerova L, Griebeler ML, Reynolds JP, Henry MR, Gharib H. Metastasis to the Thyroid Gland. *Am. J. Clin. Oncol.* 2015 Aug;38(4):338-42. PMID: 23799287
2. Chung AY, Tran TB, Brumund KT, Weisman RA, Bouvet M. Metastases to the Thyroid: A Review of the Literature from the Last Decade. *Thyroid.* 2012 Nov;22(3):258-68. PMID: 22313412
3. Yadav S, Bennani-Baiti N. Renal cell carcinoma metastasis to the thyroid: How long is long enough? *Acta Oncol.* 2014;53(9):1277-8. PMID: 25152222

4. Heffess CS, Wenig BM, Thompson LD. Metastatic renal cell carcinoma to the thyroid gland: A clinicopathologic study of 36 cases. *Cancer.* 2002 May;95(9):1869-78. PMID: 12404280
5. Sindoni A, Rizzo M, Tuccari G, et al. Thyroid metastases from renal cell carcinoma: Review of the literature. *Scientific World Journal.* 2010 Apr;10:590-602. PMID: 20364245
6. Koul H, Huh JS, Rove KO, et al. Molecular aspects of renal cell carcinoma: a review. *Am. J. Cancer Res.* 2011 Jan;1(2):240-54. PMID: 21969126
7. Zamarrón C, Abdulkader I, Areses MC, García-Paz V, León L, Cameselle-Teijeiro J. Metastases of Renal Cell Carcinoma to the Thyroid Gland with Synchronous Benign and Malignant Follicular Cell-Derived Neoplasms. *Case Rep. Oncol. Med.* 2013 Mar;1-5. PMID: 23878753
8. Medas F, Calò PG, Lai ML, Tuveri M, Pisano G, Nicolosi A. Renal cell carcinoma metastasis to thyroid tumor: A case report and review of the literature. *J. Med. Case Rep.* 2013;7:1-5. PMID: 24325865
9. Macedo-Alves D, Koch P, Soares V, Gouveia P, Honavar M, Taveira-Gomes A. Thyroid metastasis from renal cell carcinoma - A case report after 9 years. *Int. J. Surg. Case Rep.* 2015 Sep;16:59-63. PMID: 22102612
10. Sountoulides P, Metaxa L, Cindolo L. Atypical presentations and rare metastatic sites of renal cell carcinoma: A review of case reports. *J. Med. Case Rep.* 2011;5(1):429. PMID: 21888643
11. Cilengir AH, Kalayci TO, Duygulu G, Atasever RT, İnci MF. Metastasis of Renal Clear Cell Carcinoma to Thyroid Gland Mimicking Adenomatous Goiter. *Polish J. Radiol.* 2016 Dec;81:618-21. PMID: 28096905
12. Testini M, Lissidini G, Gurrado A, Lastilla G, Ianora AS, Fiorella R. Acute airway failure secondary to thyroid metastasis from renal carcinoma. *World J. Surg. Oncol.* 2008 Feb;6:4-7. PMID: 18252002
13. Riaz K, Tunio MA, Alasiri M, Elbagir Mohammad AA, Fareed MM. Renal cell carcinoma metastatic to thyroid gland, presenting like anaplastic carcinoma of thyroid. *Case Rep. Urol.* 2013 Mar. PMID: 23662243
14. Razzaq F, Alam N, Lane L. Renal carcinoma metastasis in thyroid gland mimicking a benign goiter. *Eurorad, Case* 14612, 2017. Available at: <http://www.eurorad.org/case.php?id=14612> Accessed August 10, 2018.
15. Kobayashi K, Hirokawa M, Yabuta T, et al. Metastatic carcinoma to the thyroid gland from renal cell carcinoma: Role of ultrasonography in preoperative diagnosis. *Thyroid Res.* 2015;8(1). PMID: 25802554
16. Song OK, Koo JS, Kwak JY, Moon HJ, Yoon JH. Metastatic renal cell carcinoma in the thyroid gland:

- ultrasonographic features and the diagnostic role of core needle biopsy. *Ultrasonography*. 2016 Nov;36(3):1-8. PMID: 27956733
17. Adamczewski Z, Dedecjus M, Skowrońska-Jóźwiak E, Lewiński A. Metastases of renal clear-cell carcinoma to the thyroid: a comparison of shear-wave and quasi-static elastography. *Polskie Archiwum Medycyny Wewnętrznej*. 2014;124(9):485-86. PMID: 24995474
18. Andrioli M, Persani L. Elastographic presentation of synchronous renal cell carcinoma metastasis to the thyroid gland. *Endocrine Imaging*. 2013;2(1):37-48. PMID: 24783037
19. Lee JG, Yang Y, Kim K, et al. A case of metastatic renal cell carcinoma to thyroid gland. *Chonnam Med. J*. 2011;47(2):130-3. PMID: 22111075
20. Kim Y, Lee JJ, Paik JH, Kim YK, Kim SE. Detection of Thyroid Metastasis of Renal Transitional Cell Carcinoma Using FDG PET/CT. *Nucl. Med. Mol. Imaging*. 2011 Mar;45(2):149-51. PMID: 24899995
21. Ma H, Shen G, Liu B, Yang Y, Ren P, Kuang A. Diagnostic performance of 18F-FDG PET or PET/CT in restaging renal cell carcinoma: a systematic review and meta-analysis. *Nuclear Medicine Communications*. 2017;38(2):156-63. PMID: 27824726
22. Lang BHH, Law TT. The Role of 18F-Fluorodeoxyglucose Positron Emission Tomography in Thyroid Neoplasms. *The Oncologist*. 2011;16:458-66. PMID: 22007340
23. Manohar K, Mittal BR, Kashyap R, Bhattacharya A, Singh B. Renal cell carcinoma presenting as isolated thyroid metastasis 13 years after radical nephrectomy, detected on F-18 FDG PET/CT. *Clin. Nucl. Med*. 2010;35(10):818-9. PMID: 20838298
24. Foppiani L, Massollo M, Del Monte P, Bandelloni R, Arlandini A, Piccardo A. Late-onset metastasis of renal cell carcinoma into a hot thyroid nodule: an uncommon finding not to be overlooked. *Case Rep. Endocrinol*. 2015. PMID: 25628901
25. Razek AAK, Sadek AG, Kombar OR, Elmahdy TE, Nada N. Role of Apparent Diffusion Coefficient Values in Differentiation Between Malignant and Benign Solitary Thyroid Nodules. *AJNR Am J Neuroradiol*. 2008;29(3):563-68. PMID: 18039755
26. Chin CJ, Franklin JH, Moussa M, Chin JL. Metastasis from renal cell carcinoma to the thyroid 12 years after nephrectomy. *CMAJ*. 2011 Sep;183(12):1398-9. PMID: 21242273
27. Iesalnieks I, Machens A, Bures C, et al. Local Recurrence in the Neck and Survival After Thyroidectomy for Metastatic Renal Cell Carcinoma. *Ann. Surg. Oncol*. 2015 Dec;22(6):1798-1805. PMID: 25472649
28. Takashima S, Sone S, Takayama F, et-al. Papillary thyroid carcinoma: MR diagnosis of lymph node metastasis. *AJNR Am J Neuroradiol*. 1998 Mar;19(3):509-13. PMID: 9541309
29. Bin Saeedan M, Aljohani IM, Khusaim AO, Bukhari SQ, Elnaas ST. Thyroid computed tomography imaging: pictorial review of variable pathology. *Insights Imaging*. 2016 May;7(4):601-7. PMID: 27271508
30. Nachiappan AC, Metwalli ZA, Hailey BS, Patel RA, Ostrowski ML, Wynne DM. The Thyroid: Review of Imaging Features and Biopsy Techniques with Radiologic-Pathologic Correlation. *RadioGraphics*. 2014;34(2):276-293. PMID: 24617678
31. Wunderbaldinger P, Harisinghani MG, Hahn PF, et-al. Cystic lymph node metastases in papillary thyroid carcinoma. *AJR Am J Roentgenol*. 2002;178(3):693-7. PMID: 11856700
32. Hoang JK, Lee WK, Lee M, Johnson D, Farrell S. US Features of Thyroid Malignancy: Pearls and Pitfalls. *RadioGraphics*. 2007;27(3):847-860. PMID: 17495296
33. Lee SH, Han S, Lee HS, et al. Association Between 18F-FDG Avidity and the BRAF Mutation in Papillary Thyroid Carcinoma. *Nucl Med Mol Imaging*. 2016;50(1):38-45. PMID: 26941858
34. Araz M, Çayır D. 18F-Fluorodeoxyglucose-Positron Emission Tomography/Computed Tomography for Other Thyroid Cancers: Medullary, Anaplastic, Lymphoma and So Forth. *Molecular Imaging Radionucl Ther*. 2017;26(1):1-8. PMID: 28291004
35. Lee JW, Yoon DY, Choi CS, et al. Anaplastic thyroid carcinoma: Computed tomographic differentiation from other thyroid masses. *Acta radiol*. 2008;49(3):321-27. PMID: 18365821

FIGURES

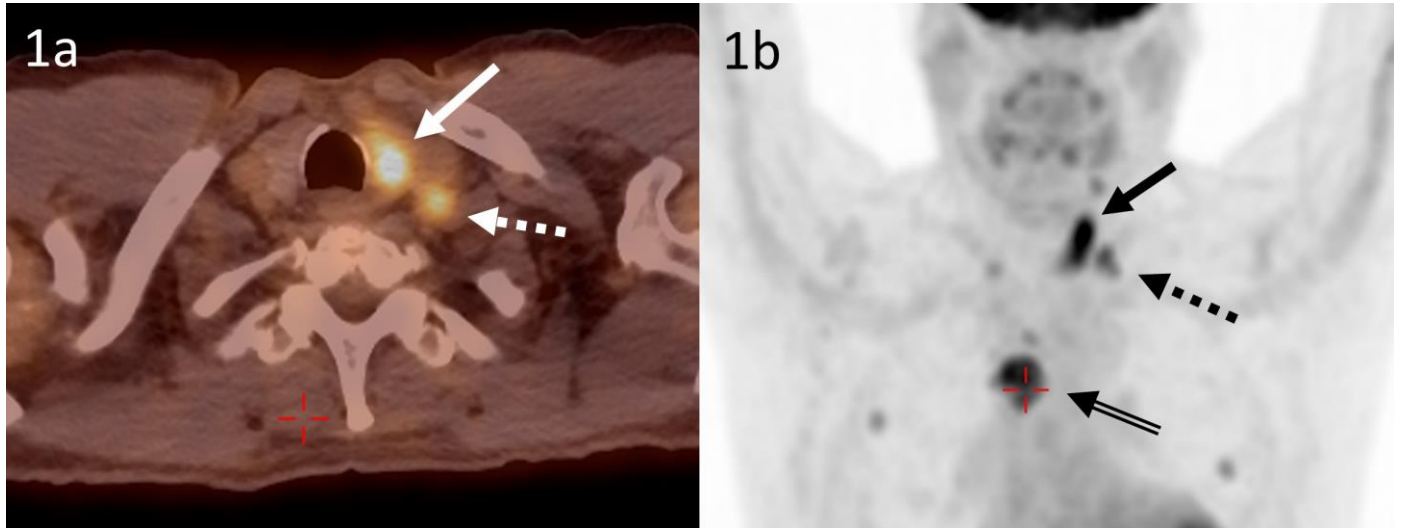


Figure 1: 66-year-old male with renal cell carcinoma status post resection.
 Findings: Positron Emission Tomography/Computed Tomography. a) Axial fused image showing a focal hypermetabolic mass (max SUV 8.6) centered within the left thyroid lobe (solid white arrow) compatible with a thyroid metastasis from primary left RCC. An adjacent left posterolateral hypermetabolic focus (max SUV 3.5) is consistent with metastatic lymphadenopathy (A: white dashed arrow). b) Maximum intensity projection showing FDG uptake at the level of the left thyroid lobe and posterolateral lymph nodes (black solid arrow and black dashed arrow respectively). An additional hypermetabolic focus (max SUV 3.3) was identified in the right upper lobe of the lung (B: striped black arrow).
 Technique: Positron Emission Tomography/Computed Tomography, 11.07 mCi F-18 FDG pharmaceutical dose, 60-minute uptake time
 a) Axial fused image, lossless 18:1 compression
 b) Maximum intensity projection, lossless 23:1 compression

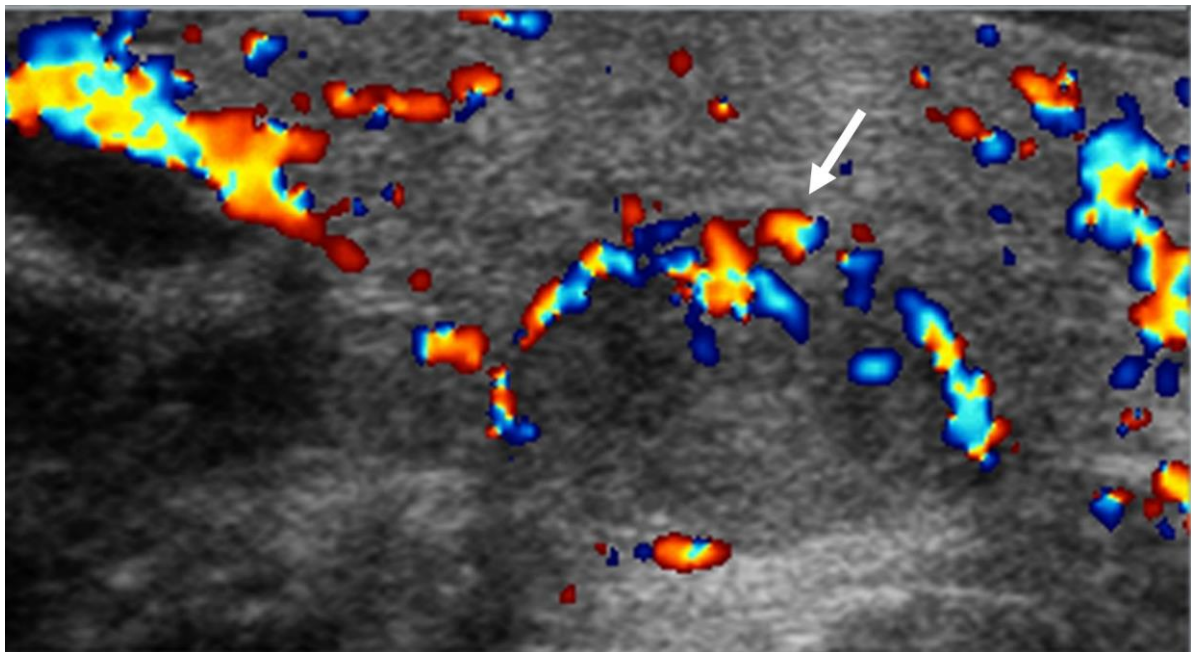


Figure 2: 66-year-old male with renal cell carcinoma status post resection.
 Findings: Heterogeneously hypoechoic nodule (solid arrow) in the left mid/lower pole measuring 3.3 x 1.6 x 1.4 cm with internal hypervascularity.
 Technique: Color Doppler ultrasonography, Siemens Acuson 15L8 - S transducer, 14 MHz

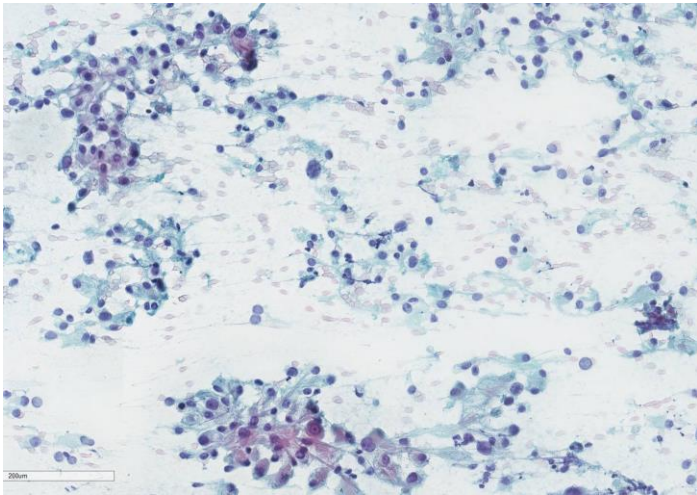


Figure 3 (left): 66-year-old male with renal cell carcinoma status post resection.
 Findings: Micrograph of pathological specimen demonstrating positive CD10 staining compatible with RCC origin.
 Technique: Light microscopy, magnification 150x, hematoxylin - eosin stain

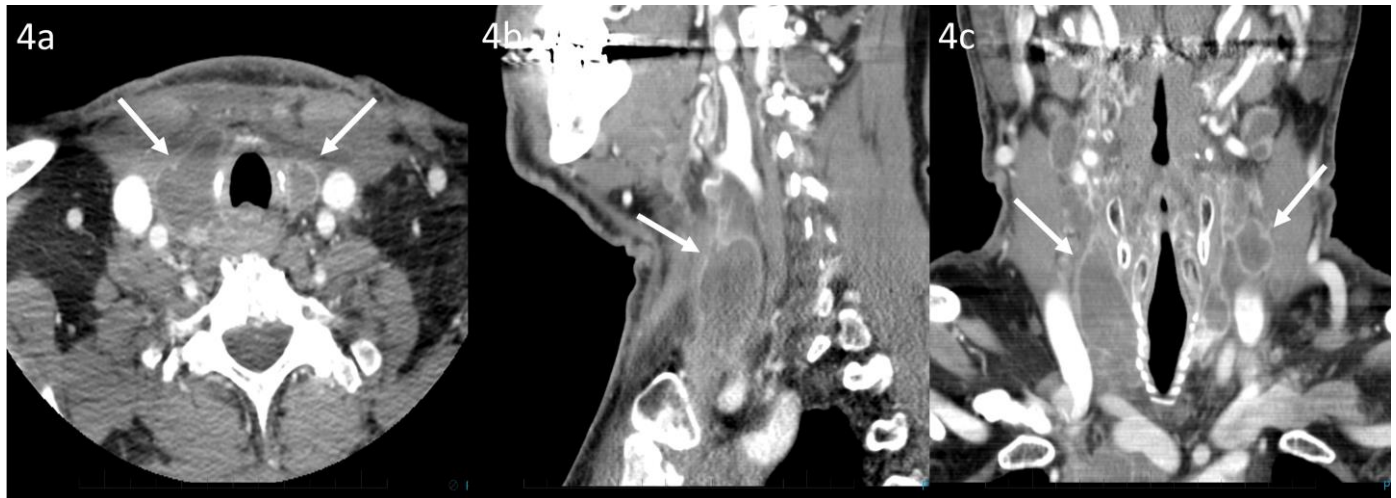


Figure 4: 66-year-old male with renal cell carcinoma status post resection.
 Findings: Computed Tomography with contrast at the level of the thyroid. a) Axial image demonstrating hypodense lesions within both thyroid lobes with irregular peripheral nodular enhancement (white arrows), more extensive on the right measuring 3.3 cm x 2.5 cm x 4.6 cm. b) Sagittal image of the right hypodense lesion with peripheral nodular enhancement c) Coronal image demonstrating the same hypodense lesions with irregular peripheral nodular enhancement (white arrows). Findings are consistent with a combination of metastatic involvement and internal necrosis of both thyroid lobes, right greater than left.
 Technique: Computed Tomography with contrast, 680 mA, 120 kVp
 a) Axial soft tissue window, 2.5 mm slice thickness
 b) Sagittal soft tissue window, 2.5 mm slice thickness
 c) Coronal soft tissue window, 3.0 mm slice thickness

Etiology	Arising from primary renal cell carcinoma
Incidence	10 – 35% of all metastases to the thyroid which make up only 1.3 – 3% of thyroid malignancies found clinically
Gender Ratio	Female: Male = 1.35:1
Age Predilection	6th and 7 th decades
Risk Factors	History of renal cell carcinoma with additional benign or malignant thyroid abnormality
Treatment	Surgical resection, immunotherapy, multi-kinase inhibitors, anti-vascular endothelial growth factor (VEGF) agents, mammalian target of rapamycin inhibitors
Prognosis	Favorable for patients that can undergo thyroidectomy. 5-year survival rate of 46% status post thyroidectomy
Findings on Imaging	<u>Ultrasound</u> : Irregular or ovoid shape, solid mass, hypoechoic, internal hypervascularity, potential “echogenic tongue” representing tumor thrombus entering the thyroid or internal jugular vein <u>Computed Tomography</u> : Hypodense with nodular, peripheral enhancement <u>Positron Emission Tomography</u> : Avid uptake of FDG

Table 1: Summary table for renal cell carcinoma metastasis to the thyroid.

	US	CT	PET
Renal cell carcinoma metastasis	Solid mass with ovoid or irregular contours, heterogenous hypoechogenicity, internal vascularity, no hyperechoic calcifications, potential echogenic protrusions into the internal jugular vein	Nonspecific appearance, central hypodensity with peripheral enhancement	Avid FDG uptake
Papillary thyroid carcinoma	Solid nodular appearance with ill-defined margins, internal vascularity, and heterogenous, hyperechoic internal microcalcifications (psammoma bodies)	Heterogenous, dense mass with occasional small internal hyperdensities representing microcalcifications, lymph node involvement	Variable FDG uptake associated with specific genetic mutations
Follicular neoplasm	Solitary, uniform hypoechoic nodule surrounded by normal thyroid tissue, poorly differentiated variants can show a poorly defined margins without normal adjacent thyroid tissue	Nonspecific, hypo - isodense mass	Increased FDG uptake with increasingly poor differentiation as glucose transporter 1 expression is up regulated
Medullary thyroid carcinoma	Solid, nodular structure with ill-defined lateral margin and extracapsular extension, coarse calcifications	Hypodense with possible hyperdense, large, coarse calcifications	Variable FDG uptake with overlap between max SUV of progressive and stable disease
Anaplastic thyroid carcinoma	Heterogenous infiltrative appearance with possible hyperechoic microcalcifications	Large, solid, infiltrative, ill-defined masses with hypodense regions marking necrosis and occasional hyperdense regions representing nodular calcification	Avid FDG uptake
Lymphoma	Diffusely heterogenous internal echogenicity, infiltrative, extracapsular extension	Diffuse heterogenous density commonly representing replacement of normal thyroid parenchyma, displacement of airway and vascular structures	Avid FDG uptake

Table 2: Differential diagnoses table for renal cell carcinoma metastasis to the thyroid.

ABBREVIATIONS

ADC = apparent diffusion coefficient
CNB = core needle biopsy
CT = computed tomography
FDG = fludeoxyglucose
FNA = fine needle aspiration
max SUV = maximum standardized uptake value
MRI = Magnetic resonance imaging
mTOR = mechanism target of rapamycin
PET/CT = Positron emission tomography/computed tomography
RCC = renal cell carcinoma
TTF 1 = thyroid transcription factor 1
VEGF = vascular endothelial growth factor

KEYWORDS

Neoplasm Metastasis; Thyroid Gland; Hypervascular Mass; Carcinoma, Renal Cell; Ultrasonography; Positron Emission Tomography Computed Tomography; Computed Tomography

Online access

This publication is online available at:

www.radiologycases.com/index.php/radiologycases/article/view/3497

Peer discussion

Discuss this manuscript in our protected discussion forum at:

www.radiolopolis.com/forums/JRCR

Interactivity

This publication is available as an interactive article with scroll, window/level, magnify and more features.

Available online at www.RadiologyCases.com

Published by EduRad



www.EduRad.org